JOURNAL OF MATERIALS SCIENCE 20 (1985) 229–236

Electron emission and acoustic emission from the fracture of graphite/epoxy composites

J. T. DICKINSON, A. JAHAN-LATIBARI, L. C. JENSEN
Department of Physics, Washington State University, Pullman, Washington 99164-2814, USA

In past studies it has been shown that the fracture of materials leads to the emission of a variety of species, including electrons, ions, neutral molecules, and photons, all encompassed by the term fracto-emission (FE). In this paper we examine electron emission (EE) from the fracture of single graphite fibres and neat epoxy resin. We also combine measurements of EE with the detection of acoustic emission (AE) during the testing of graphite–epoxy composite specimens with various fibre orientation. The characteristics of these signals are related to known failure mechanisms in fibre-reinforced plastics. This study suggests that by comparing data from AE and FE meausrements, one can detect and distinguish the onset of internal and external failure in composites. EE measurements are also shown to be sensitive to the locus of fracture in a composite material.

1. Introduction

In acquiring an understanding of the performance of composite structures, it is essential to accurately describe the processes leading up to crack formation in model composites under stress. To gain this understanding, a number of techniques have been developed for sensing damage to these materials prior to failure. Acoustic emission (AE) is an example of such a technique; it has been used successfully to detect areas of weakness in composite specimens prior to failure [1, 2]. With the aid of AE, Bailey *et al.* [3] were able to detect the location of flaws within composite components and investigate the time-dependent formation and propagation of cracks during loading. Rotem [4] was able to discriminate between different failure modes in composites by analysing amplitude intensity distributions of AE.

Recently, we have been investigating a set of physical phenomena called fracto-emission (FE) that involves the emission of particles (e.g. electrons, positive ions, neutral molecules, and photons) during and following the propagation of a crack. Most of our work has concentrated on electron emission (EE) and positive ion emission (PIE), which have been detected from a wide range of materials (see [5–16]). The results from the fracture of individual 10 μm fibres of E-glass, S-glass, and graphite [5, 11] showed the emission from these materials to be relatively intense (typically 10^8 particles cm^{-2} of cross-sectional area) and short-lived, typically decaying away in 10 to 50 μsec. The fracture of Kevlar™ fibres [15] produced multiple bursts of emission, again intense, indicating the formation and/or pull-out of individual fibrils within the strands. These bursts, approximately 50 μsec in duration, were often hundreds of microseconds apart in groups of 1 to 6.

Fracture of an unfilled epoxy (DER 332/T403, a bisphenol-type A resin) yielded relatively weak emission (typically 10^3 particles cm^{-2} of cross-sectional area) with a decay time of about 25 μsec [8]. Fracture of the filament/epoxy strands using the same epoxy resulted in significantly different emission curves [8, 14]. During fracture, the EE and PIE rise together in the form of large bursts. Immediately following separation this intense

0022–2461/85 $03.00 + .12

emission begins to decay away; the decay is very slow and lasts for many seconds. Intense emitters can yield detectable emission for as long as 2 h after fracture. As discussed elsewhere [5–14, 16, 17] we have found this behaviour to be characteristic of interfacial or adhesive failure. A model involving the physical phenomena accompanying such fracture is presented by Jensen *et al.* [13], wherein the charge separation between dissimilar materials in contact (e.g. epoxy/glass) can play a critical role.

In this paper we present initial results of EE and PIE measurements from the fracture of unidirectional graphite–epoxy composites as well as measurements from multi-directional graphite–epoxy involving a comparison of AE and EE accompanying the flexural loading of such composites.

Composite materials generally exhibit a variety of failure modes including matrix cracking, debonding, fibre breakage resulting from statistical distribution of fibre strength, delamination, and void growth [18]. Some of these events, prior to failure, may be detectable in both EE and AE. The basic requirement for detecting fracture events with FE is that the newly created fracture surfaces are in some manner in communication with the vacuum so that the particles can escape from the sample and be detected. Thus, the existence or lack of correlations between AE and EE may thus provide information useful for sorting out the mechanisms leading up to failure as well as aiding in determining if AE originates within the bulk of a sample or on its surface.

2. Experimental procedure

Unidirectional graphite–epoxy composites (provided by NASA-Ames Material Science and Application Office) made from Union Carbide Thornel 300 graphite fibres and NARMCO 5208 epoxy resin were fractured in tension. These were of very small cross-section (typically 1 to 3 mm by 0.2 mm and a gauge length of 1.5 cm. A sharp notch was made in the centre of the tension sample to encourage fracture in the region of the particle detector. Graphite–epoxy composites made from Union-Carbide Thornel 300 fibres in various NARMCO and Fiberite epoxy resins (5208, 5209, and 934) as well as neat NARMCO 5208 resin were tested in flex. The fibre directions and number of plays in these composites were $(0)_{16}$, $(\pm 45)_{16}$ and $(0, 90, 90, 0)_{16}$ with all angles measured relative to the long axis. Composite and neat resin flex samples were typically 10 cm × 1.4 cm × 0.13 cm. When tested in three-point flex a span of 4 cm and span-to-depth ratio of 30:1 was used with a strain rate of 0.064 mm sec^{-1}. Samples tested in flex contained no notch.

In addition, the EE from the fracture in tension of Thornel 300 graphite fibres was examined. The 1.5 cm long fibres were held adhesively in aluminium tabs which attached to clamps in a tensile testing apparatus.

Experiments were performed in vacuum at a pressure of 1×10^{-5} Pa. The detectors used for charged particles are channeltron electron multipliers (CEMs) which produce fast (10 nsec) pulses with approximately 90% absolute detection efficiency for electrons and nearly 100% efficiency for positive ions. The gains of the CEMs used were typically 10^6 to 10^8 electrons/incident particle. Optimum collection efficiency was sacrificed by positioning the detectors 4 cm away from the sample with a protective grid of fine metallic mesh placed between the sample and the CEM in order to protect the CEM from small pieces of graphite fibre frequently ejected from the samples under test. If these tiny "hairs" reached the front cone of the CEM it would lead to severe noise. Normal background noise counts ranged from 1 to 10 counts sec^{-1}. Standard nuclear physics data aquisition techniques were employed to count and store pulses, normally as functions of time.

Acoustic emission (AE) was detected with a PZT transducer (Acoustic Emission Technology Corporation AC175L) with a resonant frequency of 175 Hz. The bursts were typically 500 μsec in duration. The filtered and amplified signal was fed into a discriminator to eliminate background noise, and the resulting pulses were counted on a multichannel scaler. Thus the count rate displayed is determined by both the number and size of AE bursts (the number of "rings" that trigger the discriminator). To reduce the influence of mechanical AE in our experiments the mechanical supports were covered with teflon tape. Fracture of a uniform material (PMMA), which would exhibit no interlaminar shear or delamination, showed no prefracture AE in our system. Fig. 1. shows schematically the electron multipler and AE transducer arrangement used for simultaneous detection of AE and EE from the sample during flex. Load and deflection were also measured during the test to correlate AE and EE with the deformation and failure of the composite materials.

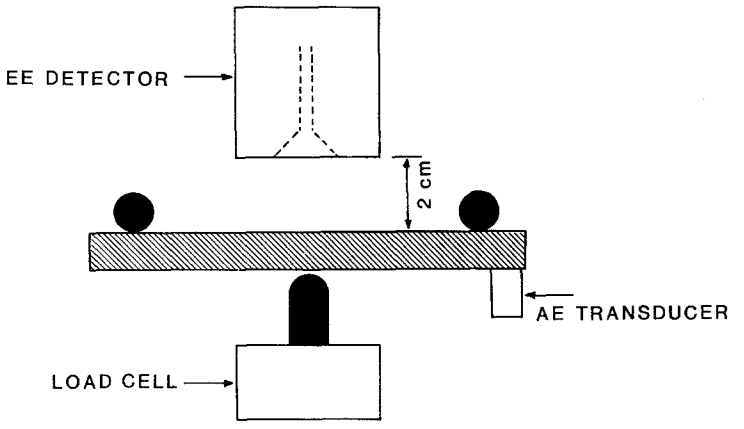

Figure 1 Schematic diagram of experimental arrangement for EE, AE, and load measurements on composite materials in flex.

3. Results and discussion

The results of EE and PIE from the fracture of two unidirectional (0°) graphite–epoxy composite samples (Thornel 300/5208) are shown in Fig. 2. The samples were 0.2 mm thick and 2 mm wide in cross-section with a small notch in the centre to cause fracture to occur in front of the detector. In general EE exceeded PIE in terms of total emission

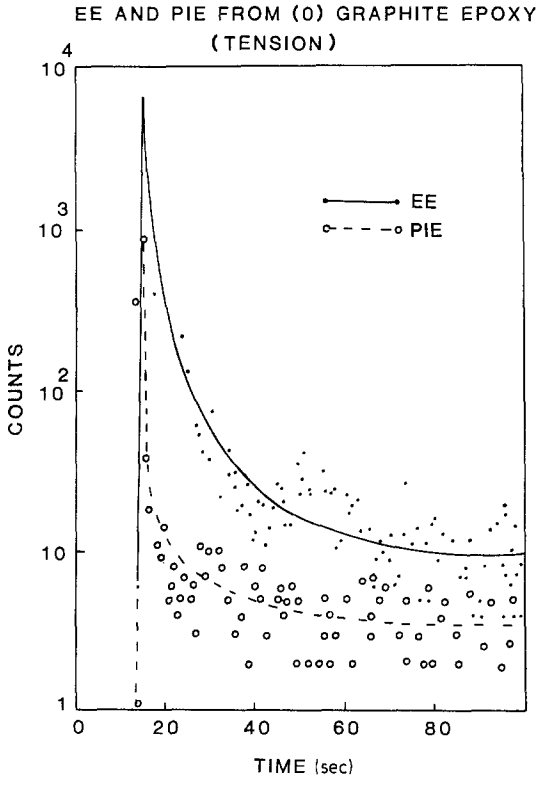

Figure 2 EE and PIE from the tensile failure of a unidirectional graphite–epoxy composite (Union Carbide Thornel 300 graphite fibres and NARMCO 5208 epoxy resin).

by 10 to 40%. Typical total EE detected counts/unit cross-sectional area (not fracture surface area) was 8×10^4 counts cm^{-2}. The resulting emission plotted on a log scale show the rapid rise during fracture and slow decay following fracture, much slower than the microsecond duration of the emission from single graphite fibres and neat resin. We also note that the decay kinetics for both EE and PIE are essentially the same, which has been observed in a number of other materials [14, 15]. Generally, simultaneous EE and PIE measurements of these decay kinetics on a number of other systems have shown them to be *exactly* the same. This has been explained by a PIE mechanism which, in fact, depends directly on the EE intensity [16].

In a number of previous experiments we have shown that the occurrence of this long lasting decay in the EE and PIE curves is due to interfacial or adhesive failure. Under this type of fracture the new sufaces created are highly charged (so-called contact charging) and the results in a highly excited surface. The electronic relaxation of this surface leads to the observed decay and appears to be rate-limited by the mobility of trapped electrons in the polymer. Thus the size and duration of this "after-emission" may serve as a measure of the extent of adhesive failure that has occurred. Further experiments that quantify the degree of such failure and compare it with the EE properties need to be carried out.

The resulting EE time distribution from the fracture of single Thornel 300 fibres, 10 μm in diameter, is shown in Fig. 3, again plotted on a log scale. The data was taken at 10 μsec/channel and represents the accumulated emission from four single fibres. On average, each fibre emitted

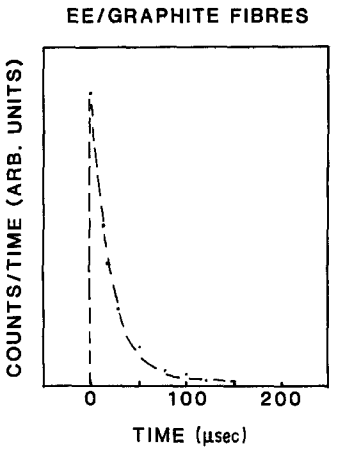

Figure 3 Accumulated time distribution of the EE from the tensile failure of single 10 μm diameter Thornel 300 graphite fibres. Four fibres were broken to obtain this distribution.

over 100 electrons. The emission rises in one channel which is consistent with a fracture event for a brittle material with such a small cross-section. Note the very rapid decay; this equivalent time constant (time to fall to $1/e$) for this decay is about 20 μsec, several orders of magnitude faster than the emission accompanying the reinforced epoxy.

Flexural testing of neat NARMCO 5208 epoxy resin was carried out measuring AE and EE simultaneously on a somewhat slower time scale than used for graphite fibre. Of primary interest was the EE resulting from fracture of the material to compare with fracture of the composite. Fig. 4 shows the resulting emission. Initial deformation produced only a few low intensity AE bursts prior to fracture, and no detectable EE. At fracture we see a burst of both AE and EE. The total number of detected counts/unit cross-sectional area is 8000 counts cm^{-2}, which is considerably smaller than the grapite/epoxy composite mentioned above. This is to be expected because the fracture of the unfilled polymer will not lead to as intense a charge separation. Similarly, the duration of the EE is much shorter due to the reduced excitation of the fracture surfaces occurring at fracture.

The AE data which we obtained for the flexural testing of graphite–epoxy composites can be generally characterized as follows: first, an initial rapid rise from zero due to the initial load applied to the specimen; second, the steady build up of the AE count rate prior to failure. Finally, a large burst followed by a drop in AE count rate at catastrophic failure.

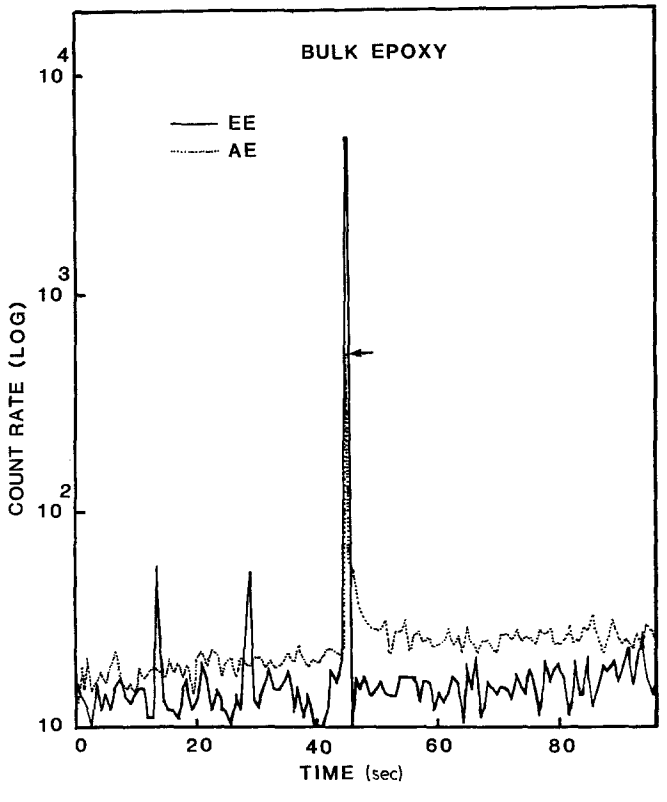

Figure 4 The EE and AE accompanying the flexural straining of NARMCO 5208 bulk epoxy resin.

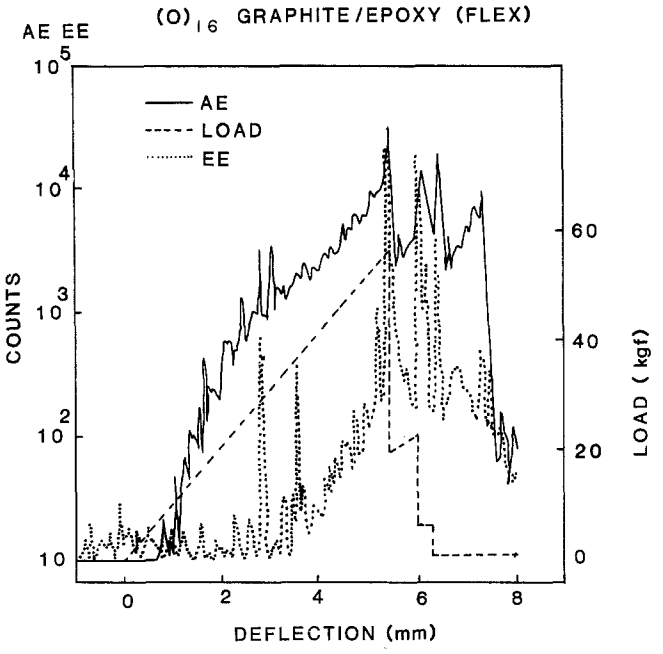

Figure 5 The EE, AE, and load accompanying the flexural straining of a $(0)_{16}$ graphite–epoxy composite. (Union Carbide Thornel 300 graphite fibres and NARMCO 5209 epoxy resin.)

Concerning AE only, it is interesting to compare our results on studies of AE from glass fibre–epoxy composites and unidirectional boron–epoxy composites tested in flex. In the case of the unidirectional glass system, Barnby and Parry [19] observed no acoustic activity prior to failure but instead observed AE only at catastrophic failure, whereas in a cross-ply (0/90) material they observed an AE build up immediately following the application of the load. For the unidirectional boron system, Fitz-Randolph *et al.* [20] have observed the steady increase of AE with deflection. The similarity of the boron and graphite systems is probably due to the fact that they are both very brittle.

In Fig. 5 we plot the AE, EE, and load against time for a $(0)_{16}$ graphite/epoxy system. The build-up of AE prior to first ply failure (where the load suddenly drops for the first time) is attributed to a combination of single-fibre fracture, and at higher loads internal delamination. Simultaneous to these measurements, a video recording was made of an image of the front surface of the specimen. The two bursts of EE in the region of 3 mm deflection were observed to occur at the same time that tiny bundles of fibres on the front surface in tension were seen to break (within the 1/60 sec time resolution of the video camera). The first EE peak has an accompanying AE peak, whereas it is not clear that the second EE peak is accompanied by a measurable AE burst above the large rising AE signal. The rise of EE that precedes the failure of the first ply is attributed to the damage occurring on the outer ply surface, perhaps involving fibre fracture, delamination, and matrix cracking. This rise in EE was seen in all (0°) specimens tested. The EE provided a much more sensitive and discriminating sensor of front surface damage (e.g. matrix cracking and small fibre bundle fracture) than the AE, primarily because of the large rising background of AE emanating from the bulk of the sample. Finally, failure of the outer ply leads to a large burst of both AE and EE similar to that observed in the fracture of the tensile specimens (Fig. 2). As additional plys failed, associated bursts of AE and EE (see Fig. 5) were frequently detectable. The EE tends to decay slowly between successive failure of the plys, which we attribute to the adhesive failure that has occurred during ply fracture.

Fig. 6 shows the AE and EE accompanying the deformation of a $(90)_{16}$ specimen in flex, plotted against time (stress–strain data were unavailable for these tests). This orientation led to early failure preceded by a rapid growth of AE, presumably due to shear. Failure occurred across the entire sample and was accompanied by the small burst of EE shown in Fig. 6. The small number of EE counts (600 counts cm^{-2} of cross-sectional area; less than 1/10 of the emission from the neat resin) and the missing tail of long lasting emission indicated that little interfacial failure occurred.

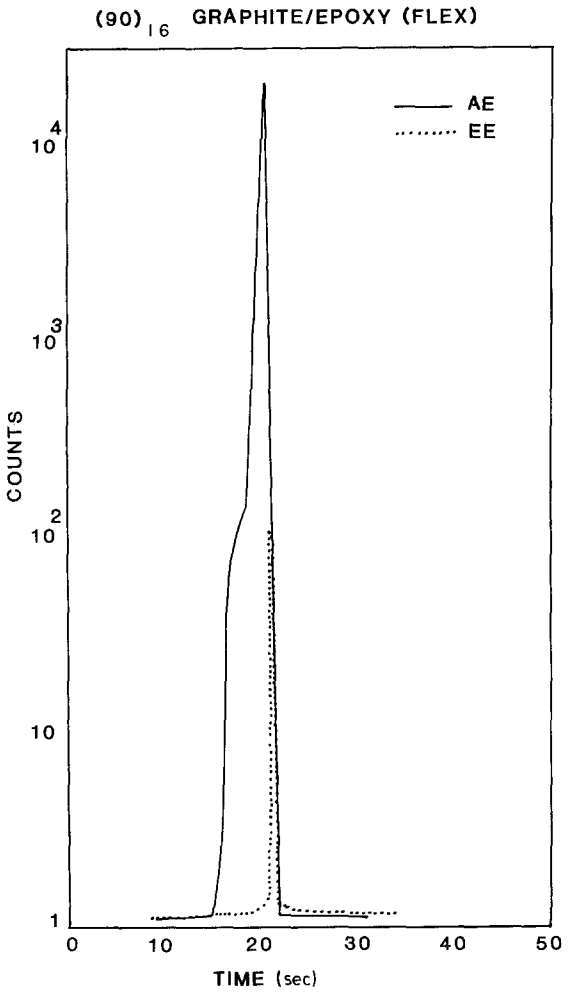

Figure 6 The EE and AE accompanying the flexural straining of a $(90)_{16}$ graphite–epoxy composite. (Union Carbide Thornel 300 graphite fibres and NARMCO 5208 epoxy resin.) This curve is plotted against time because stress–straining information was not available at the time of testing. The strain rate was 0.064 mm sec^{-1}.

SEM analysis of the fracture surface showed that failure was in fact in the *epoxy matrix* and thus produced an emission curve much like the fracture of bulk resin. The reduced emission relative to the neat resin may be due to the weakness of the material in this particular direction, thus less energy dissipated at the crack tip. These results suggest that the shape and intensity of the EE curve may provide useful information on the quality of the fibre–matrix bonding and its influence on the path of fracture.

In the case of $(\pm 45)_{16}$ specimens stressed in flex, (the reinforcement fibres are at $\pm 45^\circ$ to the long axis) interlaminar fracture is expected to be the main failure mechanism. Soon after the load is applied, as seen in Fig. 7, the AE grows rapidly due to interlaminar shear, slowly levelling off at a high level due to continual relative motion of the plys. The load curve shows curvature due to continual loss of modulus. The average EE count rate rises slightly above the background level with frequent bursts of EE suggestive of small fracture events. Since most of the damage to the sample is occurring internally, the EE observed is probably due to fracture events on the edges of the sample.

The AE and EE data from a $(0/90/90/0)_{16}$ specimen are shown in Fig. 8. Here again we note AE build-up prior to failure, attributed to large interlaminar shear deformation, which then drops with the load upon failure. Model calculations on these materials under our load conditions, performed at NASA-Ames Research Center by O. Isahi, showed that initial failure would occur in the second (interior) 90° ply. Video observation showed that this was accompanied by simultaneous failure of the exterior 0° ply. The lack of EE prior to failure is again due to the internal nature of the damage that is occurring. Once the *outer* ply fails, however, we observe the burst of EE. Subsequent double-ply failure (first a 90 then a 0) was also observable in both AE and EE. We hope to soon measure the time interval between the rise in AE accompanying the failure of the first 90° ply and the EE burst (which we think is due to the failure of the exterior 0° ply), and thereby determine the actual time between failure of these two plys.

4. Conclusions

We have presented a number of preliminary results on the emission of particles, primarily electrons, accompanying the deformation and /or fracture of single graphite fibres, neat epoxy, and graphite/epoxy composites. We have shown that in conjunction with AE and load measurements we are able to detect evidence of interfacial failure as well as predominately cohesive failure events, the breaking of small fibre bundles and matrix cracking at the composite surface, and identify acoustic events which lack a corresponding EE signal and are therefore due to internal failure. In general, the use of EE and possibly other FE signals such as photon emission, neutral emission, and even radio-frequency electromagnetic radiation accompanying the deformation and fracture of composites will allow more details of failure mechanisms and composite characterization to be obtained. FE

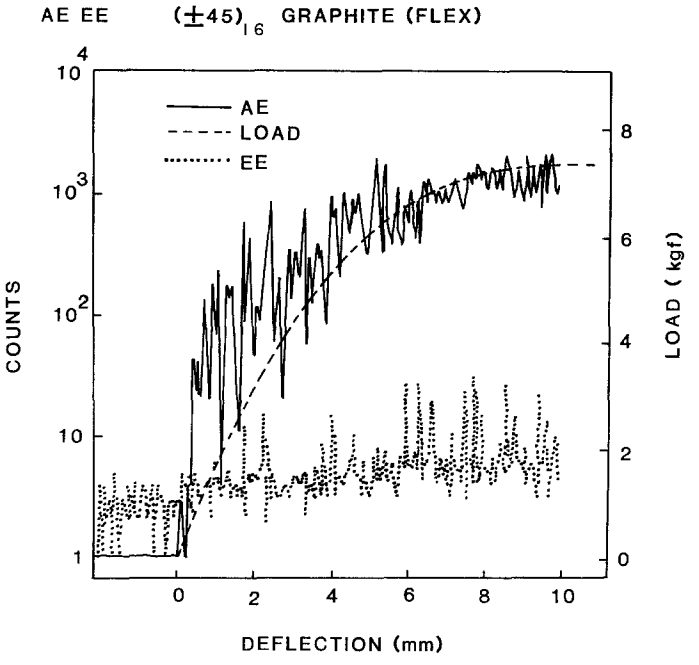

Figure 7 The EE, AE, and load accompanying the flexural straining of a 16 ply (± 45) graphite–epoxy composite. (Union Carbide Thornel 300 graphite fibres and NARMCO 5208 epoxy resin.)

potentially can assist in the interpretation of AE and also provide a independent probe of the micro-events occurring prior to failure. Finally, we have shown that EE is sensitive to the locus of fracture (cohesive fracture in the matrix vs interfacial failure). Obviously, considerable work will be required to fully utilize FE as a method for studying the early stages of fracture and failure modes in fibre-reinforced composites.

Acknowledgements

We wish to thank our Washington State University colleagues E. E. Donaldson and R. V. Subramanian for their helpful discussions and S. K. Bhattacharya

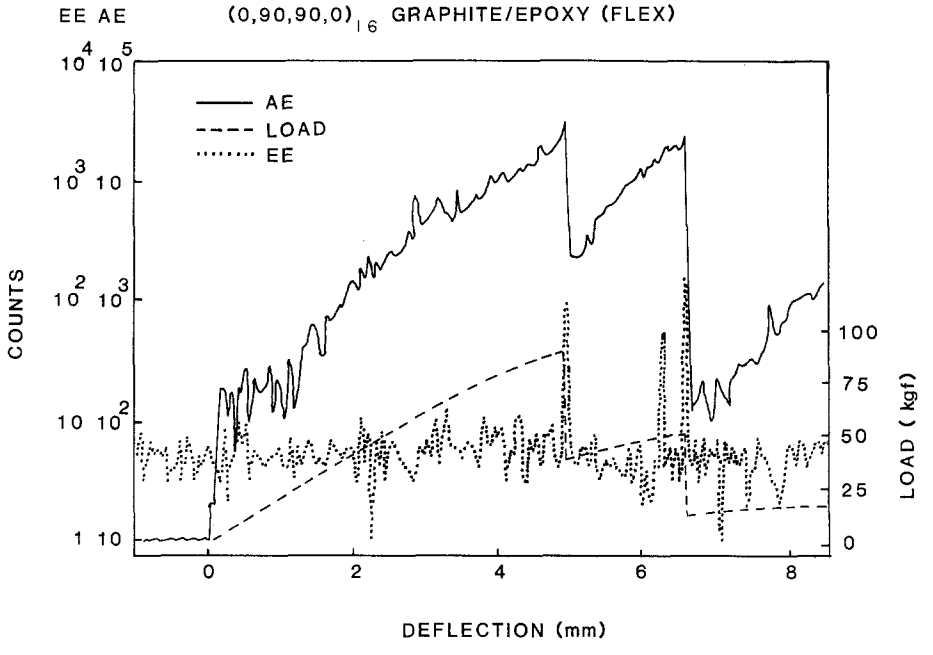

Figure 8 The EE, AE, and load accompanying the flexural straining of a 16 layer, cross-ply (0, 90, 90, 0) degree graphite–epoxy composite. (Union Carbide Thornel 300 fibres and Fiberite 934 epoxy resin.)

for his assistance. We are also appreciative of interest and advice from O. Ishai, A. Gray, and L. C. Clements of the NASA-Ames Research Center, and give particular thanks to Dr Ishai for his assistance in calculations of the mechanical behaviour of our specimens.

This work was supported by the NASA-Ames Research Center, McDonnell Douglas Independent Development Program, the National Science Foundation (Grant DMR-8210406), Sandia National Laboratories, and a grant from the M. J. Murdock Charitable Trust.

References

1. I. G. SCOTT and C. M. SCALO, NDT International, April (1982) p. 75.
2. R. HILL, *ibid.* April (1977) p. 63.
3. C. D. BAILEY, S. M. FREEMAN and J. M. HAMILTON Jr, *Mater. Eval.* (August) (1980) 21.
4. A. ROTEM, *Fiber Sci. Tech.* **10** (1977) 102.
5. J. T. DICKINSON, E. E. DONALDSON and M. K. PARK, *J. Mater. Sci.* **16** (1981) 2897.
6. J. T. DICKINSON and L. C. JENSEN, *J. Polymer Sci. Polymer Phys Ed.* **20** (1982) 1925.
7. J. T. DICKINSON, M. K. PARK, E. E. DONALDSON, and L. C. JENSEN, *J. Vac. Sci. Technol.* **20** (1982) 436.
8. J. T. DICKINSON, L. C. JENSEN, and M. K. PARK, *J. Mater. Sci* **17** (1982) 3173.
9. *Idem, Appl. Phys. Lett.* **41** (1982) 443.
10. *Idem, ibid.* **41** (1982) 827.
11. H. MILES and J. T. DICKINSON, *ibid.* **41** (1982) 924.
12. J. T. DICKINSON, L. C. JENSEN and A. JAHAN-LATIBARI, *Rubber Chem. Technol.* **56** (1983) 927.
13. J. T. DICKINSON, Fracto-Emission Accompanying Adhesive Failure, in "Adhesive Chemistry–Developments and Trends", edited by L. H. Lee (Plenum New York) to be published.
14. J. T. DICKINSON, A. JAHAN-LATIBARI and L. C. JENSEN, Fracto-Emission from Fiber-Reinforced and Particulate Filled Composites, in "Polymer Composites and Interfaces", edited by N. G. Kumar and H. Ishida (Plenum, New York) to be published.
15. L. C. JENSEN, J. T. DICKINSON and A. JAHAN-LATIBARI, *J. Mater. Sci.* **19** (1984) in press.
16. J. T. DICKINSON, L. C. JENSEN and A. JAHAN-LATIBARI, *J. Vac. Sci. Technol.* **A2** (1984) 1112.
17. J. T. DICKINSON and L. C. JENSEN, *J. Polymer Sci. Phys.* Ed. to be published.
18. C. K. H. DHARAN, *J. Mater. Eng. Tech.* **100** (1972) 233.
19. J. T. BARNBY and T. PARRY, *J. Phys. D Appl. Phys.* **9** (1976) 1919.
20. J. FITZ-RANDOLPH, D. C. PHILLIPS, P. W. R. BEAUMONT and A. S. TETELMAN, *J. Mater. Sci.* **7** (1972) 289.

Received 23 January
and accepted 13 March 1984